Performance of ATM Networks Under Hybrid ARQ/FEC Error Control Scheme

Maan A. Kousa, *Member, IEEE,* Ahmed K. Elhakeem, *Senior Member, IEEE,* and Hui Yang

***Abstract*— In ATM networks, fixed-length cells are transmitted. A cell may be discarded during the transmission due to buffer overflow or detection of errors. Cell discarding seriously degrades transmission quality. This paper analyzes a hybrid automatic repeat request/forward error control (ARQ/FEC) cell-loss recovery scheme that is applied to virtual circuits (VC's) of ATM networks. FEC is performed based on a simple single-parity code, while a Go-Back-N ARQ is employed on top of that. Both throughput efficiency and reliability analysis of the hybrid scheme are presented. In the process we investigate the interactive effects of the network parameters (number of transit nodes, traffic intensity, ARQ packet length, ...) on the performance. The analysis provides a method for optimizing the FEC code size for a given network specification.**

***Index Terms*— ARQ/FEC, ARQ packet, ATM networks, Go-back-N, throughput efficiency, traffic intensity, virtual circuits.**

I. Introduction

THERE HAS been great interest lately in the utilization of ATM technology for both wired and wireless networks, and it has been adapted as the platform for Broadband Integrated Service Digital Networks (B-ISDN) [1], [2].

The basic unit in ATM networks is the cell. A cell consists of a header section and a payload (data) section. The header (5 bytes) is checked for errors at transit nodes with the aid of a CRC-8 code. If a header is found to be in error, the cell is discarded. ATM adaptation layer (AAL) types 2, 3, or 4 allow for checking the payload, as well using CRC-10 code [3]. A cell may also be discarded because of buffer overflow.

Cell discarding seriously degrades transmission quality and is considered one of the major problems in ATM-based networks. Because high quality and reliability are essential in B-ISDN, the employment of error detection and/or error correction for ATM networks to control the cell-loss rate has gained a lot of attention [3]–[7].

In [3], a cell-recovery method to be applied to the virtual paths (VP's) of ATM networks was proposed. The method consists of cell-loss detection (CLD) and lost cell regeneration. The data cells are arranged in a matrix of $(M-1)\times(N-1)$ cells. Each row of data cells is terminated by a specially designed cell, called a CLD cell, while each column is terminated by a parity cell formed based on a single-parity check code. Decoding is performed in two steps. Lost cells are detected by row-wise operations with the aid of the CLD cell at the end of each row. Next, cells marked lost are regenerated by column-wise operations with the aid of the parity cell at the end of each column. The scheme in [3] was slightly modified in [4] to extend the row size of the coding matrix and thus make the scheme more robust to burst cell loss. For applications that are not time-sensitive, automatic repeat request (ARQ) schemes prove to be more reliable than forward error correction FEC schemes. However, for high-speed networks, ARQ schemes may result in low throughput efficiency and excessive storage requirement. Hybrid ARQ/FEC schemes help in improving throughput efficiency and reducing the storage requirements [5].

In this paper, we analyze the performance of a hybrid ARQ/FEC coding scheme over ATM networks. While cells are checked at the VP terminals (hop-by-hop), FEC and ARQ are only applied to the VC (end-to-end). For FEC, we adopt the coding matrix technique in [3] because of its simplicity. However, to minimize the processing delay, decoding will only be carried out at the end terminal. On top of that, a Go-Back-N (GBN) ARQ scheme will be utilized at the transport layer. The coding scheme is depicted in Fig. 1.

It was assumed in [3] that the transmission lines are optical fibers, which have negligible bit error rate (BER). In some situations, like those of wireless ATM, higher BER's are encountered. The effect of channel errors on cell-loss rate and cell-error rate (the probability that a received cell is erroneous) is considered here.

The proposed hybrid scheme will be evaluated in terms of the residual (post-decoding) cell-loss rate, throughput efficiency, and reliability of the received data. We will consider the case when only the header is CRC-protected and the case when both the header and the payload are CRC-protected. We will also consider performance with or without ARQ. All relevant system parameters (traffic intensity, number of hops, ARQ packet size, queuing-buffer size, ...) are accounted for and their effects on system performance are studied. Based on that, the size of the coding matrix will be optimized for a given network description.

The rest of the paper is organized as follows. The coding structure is described in Section II, whereas performance analysis is furnished in Section III. Results are presented and discussed in Section IV. A few case studies are included in Section V. Section VI concludes with observations and remarks.

Manuscript received July 29, 1997; revised June 16, 19998, January 6, 1999, and May 19, 1999; approved by IEEE/ACM TRANSACTIONS ON NETWORKING Editor M. Murata.

M. A. Kousa is with the Electrical Engineering Department, King Fahd University of Petroleum and Minerals, Dhahran 31261, Saudi Arabia (makousa@kfupm.edu.sa).

A. K. Elhakeem and H. Yang are with the ECE Department, Concordia University, Montreal, P. Q. H3G 1M8, Canada (ahmed@ece.concordia.ca; huiyang@nortelnetworks.com).

Publisher Item Identifier S 1063-6692(99)09715-0.

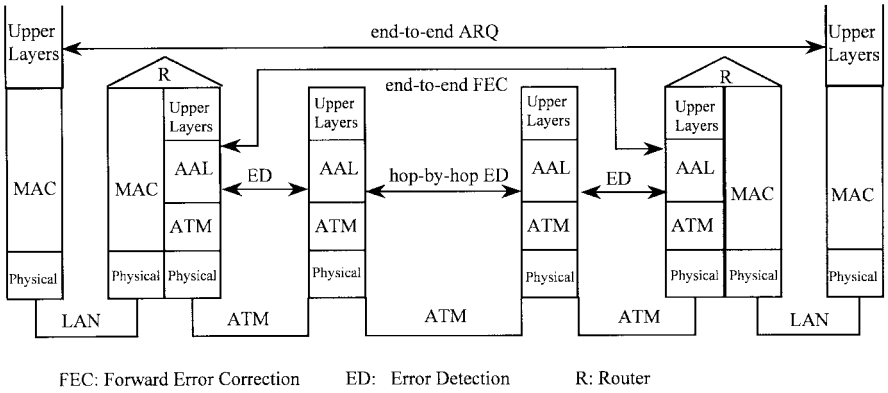

Fig. 1. Illustration of the hybrid ARQ/FEC scheme in the LAN/ATM interconnection.

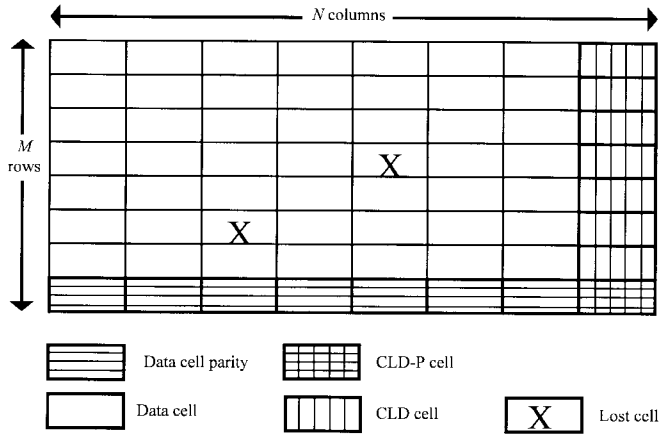

Fig. 2. Coding matrix.

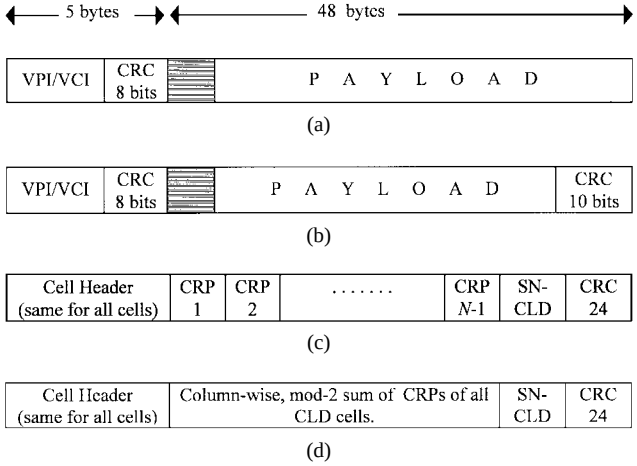

Fig. 3. The format of the various cell types used in the coding matrix. (a) Data cell when only the header is protected. (b) Data cell when both header and payload are protected. (c) CLD cell. (d) CLD-P cell.

II. Coding Structure

For FEC, we adopt the coding matrix scheme in [3] because of its simplicity and small processing time. However, in contrast to [3], encoding and decoding are only applied end-to-end at the AAL level of the source and destination ATM nodes. The objective of FEC is to regenerate cells that were lost either because they were discarded earlier due to detected channel errors or because of buffer overflow at any intermediate node.

A. Encoding

Fig. 2 shows the structure of the matrix. Data cells are arranged in $M-1$ rows and $N-1$ columns. An Nth column is formed from special cells, called cell-loss-detection (CLD) cells, that aid in detecting lost cells, while an Mth row is formed from parity cells that aid in recovering the lost cells. The most bottom right cell is a CLD parity (CLD-P) cell that is used for CLD cell recovery. Once the matrix is completed, its constituting cells are transmitted row by row. All cells in the matrix carry the same header. The four cell types that appear in the matrix are constructed as follows.

1) *Data cell*: a standard ATM cell consisting of a payload and a header. Two cases are considered here: when only the header is protected by CRC-8, and when the payload is also protected by CRC-10. The corresponding formats are shown in Fig. 3(a) and (b).
2) *CLD cell*: consists of the header followed by $N-1$ cell recognition patterns (CRP) corresponding to the $N-1$ data cells in the row, 1 byte for the sequence number (SN) of the of CLD cell (SN-CLD), and CRC-24 calculated over the $N-1$ CRP's and SN-CLD fields of this cell [3]. The SN-CLD is an identification given to each CLD cell to help discover lost CLD cells. An 8-bit SN-CLD is sufficient for a coding matrix of up to 256 columns. The format of a CLD cell is shown in Fig. 3(c).

   It is worth noting that although the FEC coding scheme is applied to VC's and not to VP's as in [3], it may still be necessary to use CLD cells to detect lost cells and not rely on the SN's assigned to data cells as in the standard cell format. This is because, in many applications, only priority cells are protected by FEC, and therefore cells in a row may not be in sequence, thus necessitating the advent of another SN related to the matrix.
3) *Parity cell*: the bottom cell of each data cell column. It is formed as the module-2 addition of all data cells in the column.
4) *CLD-P cell*: the most bottom-right cell in the matrix, and is calculated by module-2 addition of all CLD cells, as shown in Fig. 3(d).

It should be noted that in the last two types mod-2 addition is applied only to the payload segments, except for the field of SN. SN bits of parity cells (bottom row) are assigned in sequence.

B. Decoding

At the receiving node, the received cells are arranged in the $M \times N$ matrix format. First, the last column, consisting of CLD cells, is examined. Once a CLD cell is found to be missing, as per the absence of its SN, it is replaced by an all-zero cell. Performing module-2 addition of all cells in the last column, including the CLD-P cell, recovers the lost CLD cell. Next, each row is examined to check if any of its data cells is lost. The identity of lost data cells is found by comparing the CRP field of each data cell to the corresponding CRP field in the CLD cell of the corresponding row. Lost parity cells (bottom row) are easily identified by gaps in there SN's. A dummy all-zero cell is substituted instead of the lost cell. Once again, performing module-2 addition of cells in that column recovers the lost cell.

The above recovery process works well if there is one lost cell per column. If it is found that more than one cell is lost per column, the recovery process terminates completely or partially, as will be elaborated on in the coming analysis. Any remaining lost cells will be delivered to the upper layer where ARQ takes place.

A GBN-ARQ scheme, incorporating a powerful error-detection code, checks the validity of the data coming from the FEC decoding process. Note that unrecovered lost cells, being substituted by all-zero, appear as erroneous cells for the ARQ error-detection code. A retransmission is requested if a packet (formed of few cells) is found to be in error.

III. Performance Analysis

In the following, we evaluate the overall throughput efficiency and probability of error for the hybrid coding scheme described above.

A. Pre-Decoding Probabilities

Consider the outcome of processing a cell at h intermediate nodes, including the destination node. At these nodes, the header or header and payload are checked for errors; if errors are detected in either segments the cell is discarded. This adds to the possible cell discarding due to the intermediate buffer overflow.

Denoting, for $i = 1, 2, \cdots, h$:

- f_i = probability of cell loss due to buffer overflow at node i
- p_i = bit error probability on the physical wireless or terrestrial network of the ith hop
- n = number of bits of the payload
- n' = number of bits of the header
- c = cell size in bits $= n + n'$.

The probability $P_{c,i}$ that the cell survives both physical layer errors and buffer loss at the ith node is given by

$$P_{c,i} = (1 - p_i)^c (1 - f_i). \tag{1}$$

On the other hand, a cell is received in error when the cell encounters no buffer loss and the CRC failed to detect the errors. The probability of this event, $P_{e,i}$, is given by

$$P_{e,i} = (1 - f_i)\{P_{u,i} + P'_{u,i} - P_{u,i}P'_{u,i}\} \tag{2}$$

where $P_{u,i}$ and $P'_{u,i}$ are the undetected error probabilities of the payload and the header, respectively. When no CRC coding is applied to the payload, the undetected error probability is given by

$$P_{u,i} = 1 - (1 - p_i)^n. \tag{3}$$

On the other hand, if AAL types 2–4 are employed, the last 10 bits of the payload may be used as CRC field for error detection over the payload. The undetected error probability is then a function of the bit error probability of the hop and the CRC code employed. The exact calculation of the undetected error probability requires the knowledge of the weight distribution of the code, which is unknown for most codes. It is a general trend for researchers to resort to upper bounds in evaluating the undetected error probability P_u. An upper bound that is widely assumed because of its simplicity is $P_u \leq 2^{-d}$ where d is the number of the check digits [8]. Therefore, the undetected error probability of the payload when it is protected is upper bounded by

$$P_{u,i} \leq 2^{-10}. \tag{4}$$

Similarly, the undetected error probability of the header is

$$P'_{u,i} \leq 2^{-8}. \tag{5}$$

The probability that the cell is lost is then given by

$$P_{l,i} = 1 - P_{c,i} - P_{e,i}. \tag{6}$$

A typical cell traversing the h ATM nodes enroute to destination would repeat the outcomes in (1)–(6) h times. Assuming that all hops are identical on the average, i.e., have the same bit error probability, the subscript i may be dropped and the average probabilities at the destination node (before decoding) can be written as

$$\overline{P}_c = P_c^h \tag{7}$$

$$\overline{P}_e = \sum_{j=1}^{h} \binom{h}{j} P_e^j P_c^{h-j} \tag{8}$$

$$\overline{P}_l = 1 - \overline{P}_c - \overline{P}_e. \tag{9}$$

In deriving (7)–(9), the independence of all events was assumed.

B. Post-Decoding Probabilities

Next, we evaluate the modifications of the probabilities given in (7)–(9) due to using the FEC matrix decoding. Consider first the recovery of the lost data cells and data parity cells, assuming all CLD cells are present. It is easily seen that exactly one lost cell per column could be recovered, but two or more lost cells lead to unrecoverable cell loss. Therefore, the

cell-loss probability after decoding (i.e., the residual cell-loss probability) is

$$E_1 = \frac{1}{M} \sum_{j=2}^{M} j \binom{M}{j} (\overline{P}_l)^j (1-\overline{P}_l)^{M-j}. \quad (10)$$

Now consider the case of lost cells in the CLD column. The CLD-P cell can compensate for no or only one CLD lost cell. In both cases the unrecoverable cell-loss probability is given by (10). However, If there is more than one lost cell, the decoder does not attempt any recovery operations and the whole matrix of data cells is immediately delivered to the upper ARQ layer as it was received. Therefore, the probability of lost data cell for this scenario is given by

$$E_2 = \frac{1}{M} \sum_{j=2}^{M} j \cdot \binom{M}{j} (\overline{P}_l)^j (1-\overline{P}_l)^{M-j}. \quad (11)$$

In each decoding matrix we have M CLD cells and $M(N-1)$ data cells, including parity cells in both. Since cell errors are equally likely to occur anywhere within the matrix, the probability that a lost cell hits the data cells (the first $N-1$ columns) and the probability that a lost cell hits the CLD cells (the last column) are respectively $M(N-1)/MN$ and M/MN. The cell-loss probability in (10) takes place when the lost cells are confined to the data section, or when zero or one CLD cells is lost, whereas the cell-loss probability in (11) takes place when two or more CLD cells are lost. This translates to the following post-decoding average cell-loss probability P_L:

$$P_L = \left\{ \frac{N-1}{N} + \frac{1}{N} \sum_{j=0}^{1} \binom{M}{j} (\overline{P}_l^*)^j (1-\overline{P}_l^*)^{M-j} \right\} \cdot E_1 + \left\{ \frac{1}{N} \sum_{j=2}^{M} \binom{M}{j} (\overline{P}_l^*)^j (1-\overline{P}_l^*)^{M-j} \right\} \cdot E_2. \quad (12)$$

The probabilities marked $(^*)$ are evaluated for a CLD cell (where its nonheader segment is protected by CRC-24).

The above analysis was carried under the assumption of random cell loss in each column. However, the analysis is also valid for bursts of lengths shorter than N cells. If one recalls that cells are transmitted row-by-row and decoded column-by-column, the matrix effectively acts as an interleaver of depth N and, as a result, bursts of N or less lost cells are perfectly randomized. For large row size and moderate network traffic. it can be assumed that most burst losses are randomized. The validity of this assumption was checked by comparing the post-decoding cell-loss rate in (12) to that based on the Gilbert model analyzed in [3], when both models are subject to the same pre-decoding average cell-loss rate $\overline{P}_l$. For $N = 17$ and $q = 0.2$ (q expresses the conditional probability of a cell discard following a cell discard). the two approaches yield essentially the same values for P_L. The value $q = 0.2$ models a moderate input traffic [3].

Next, let us calculate the post-decoding probability that the cell is correct, P_C, and the post-decoding probability that the cell is in error, P_E. When a lost cell is recovered, it will be correct if all the other $(M-1)$ cells in the column are correct, otherwise it is assumed wrong. The post-decoding probabilities are therefore obtained by modifying the pre-decoding probabilities in (7) and (8) as follows:

$$P_C = \overline{P}_c + (\overline{P}_c)^{M-1}(\overline{P}_l - P_L) \quad (13)$$

$$P_E = \overline{P}_e + [1-(\overline{P}_c)^{M-1}](\overline{P}_l - P_L). \quad (14)$$

Note that $P_C + P_E + P_L = 1$.

C. Invoking GBN-ARQ

Now consider a packet B at the ARQ layer. A packet is formed from the payloads of r cells. There is no header at this layer. Define:

- B_C = the probability that the packet is correct
- B_E = the probability that the packet contains undetectable errors
- B_L = the probability that the packet contains lost cells
- B_D = the probability that the packet contains detectable errors.

The packet will be accepted and delivered to the user when it is correct, or when it contains undetectable errors. Otherwise, it will be retransmitted. Therefore, the probability of retransmission B_R is given by the sum of B_D and B_L. It can easily be seen that

$$B_C = (P_C)^r \quad (15)$$

$$B_E \leq 2^{-m} \quad (16)$$

$$B_R = 1 - B_C - B_E. \quad (17)$$

In (16), m represents the number of check digits for the ARQ system used to detect the errors in the packet B. We have set $m = 32$, as in [7]. This will guarantee an undetected error probability below $2^{-32} \approx 2 \times 10^{-10}$. Equation (16) implies that the only residual errors left in the packet are those which are not detectable by the error detecting code employed by the ARQ protocol, independent of the undetectable errors passed from the previous error detection at the cell level.

The ultimate probability of delivery error P, which is a measure of the reliability of the system, and the net throughput efficiency η, of the GBN-ARQ are given by [9]

$$P = \frac{B_E}{B_E + B_C} \quad (18)$$

$$\eta = \alpha \cdot \frac{1-B_R}{1+2aB_R} \quad (19)$$

where α is the ratio of the number of information bits to the number of total bits, transmitted per second. That is

$$\alpha = \begin{cases} \left\{ \dfrac{(M-1)(N-1)}{M \cdot N} \right\}, & \text{if only header is protected} \\ \left\{ \dfrac{(M-1)(N-1)}{M \cdot N} \cdot \dfrac{(c-10)}{c} \right\}, & \text{if both header and payload are protected} \end{cases} \quad (20)$$

The effect of the number of check bits m on α has been ignored because m is extremely small compared to the packet

size. In other words, the rate of the error-detecting code employed in ARQ is essentially 1.

The factor a in the denominator of (19) is the user end-to-end propagation delay in packets given by

$$a = \frac{h\tau}{T_P} + 2\left(\frac{MN}{2}\right)\left(\frac{cT_b}{r.T_P}\right) = \frac{h\tau}{T_P} + \frac{MN}{r^2} \qquad (21)$$

where τ is the one-way propagation delay and T_b and T_P are the bit length and the packet length, respectively, in seconds $(T_P = r.c.T_b)$. The first term in (21) is due to the one-way propagation delay over h ATM hops, while the second term is due to the matrix-encoding/decoding storage delay at source and destination nodes. Encoding/decoding processing at the end nodes and CRC processing times at intermediate nodes were neglected in the above calculations.

D. Buffer Overflow

We proceed next to the evaluation of the probability of buffer overflow at a certain node. For convenience, we assume a simple M/M/1/K node buffer, where each node multiplexes its own traffic (from its own LAN or LAN's) and the passing-by transit traffic.

Let the intrinsic (pure data) traffic intensity be ρ_0. This traffic intensity is magnified by the CRC codes, the parity cells of the matrix and the ARQ retransmissions. Since all these factors are accounted for in η, the inflated traffic intensity ρ is given by

$$\rho = \frac{\rho_0}{\eta} \qquad (22)$$

The reduction in traffic at a node due to dropped cells at earlier nodes on the VP is neglected. For an M/M/1 buffer of size K and traffic intensity ρ, the probability of overflow is then given by

$$f_i = \frac{(1-\rho)\rho^K}{1-\rho^{K+1}}. \qquad (23)$$

IV. Results and Discussion

The performance of the hybrid coding scheme was evaluated for the following system specifications: $h = 3, M = 17, N = 17, r = 4, K = 16, \rho = 0.5$, transmission rate $= 150$ Mb/s and $\tau = 1$ msec. Unless stated otherwise, the above values are assumed. Subtitles are added for clarity.

A. Cell-Loss Recovery

Fig. 4 provides a good indication of the power of the FEC matrix. It shows that a large percentage of the lost cells were recovered, which results in reducing the cell-loss rate by up to three order of magnitudes for $p < 10^{-6}$. The figure also shows that most of the recovered cells are correct, yielding a post-decoding error rate that is very close to the pre-decoding error rate.

B. Pure FEC Systems

Fig. 5 illustrates the cell-error performance when no ARQ retransmission is used. Such systems are appropriate for delay-sensitive traffic. Two sets of curves are shown, one for the case when the payload is not checked (referred to as Case 0) and the other for the case when the payload is checked with CRC-10 (Case 1). The results show that, although the cell-loss rate increases when the payload is checked, the overall probability that a received cell is not correct (i.e., $P_E + P_L$), which is of concern to the end user, is significantly reduced. The cost of this improvement is a slight reduction in throughput efficiency by $10/424 \approx 0.024$, due to employing CRC-10.

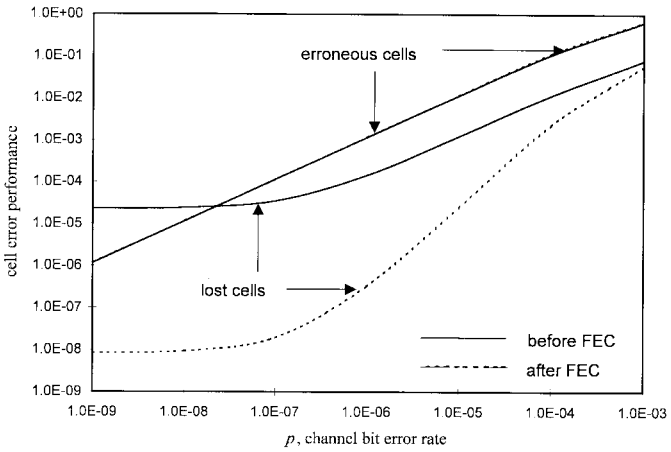

Fig. 4. Performance of the cell-recovery matrix.

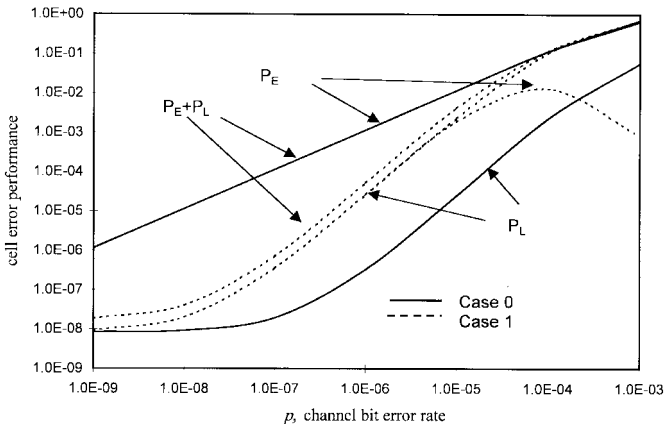

Fig. 5. Effect of payload checking on system performance for delay-sensitive traffic (no ARQ).

C. Traffic Intensity and Throughput Efficiency

The rest of the analysis applies to the case when a GBN-ARQ scheme is invoked. A CRC-32 code is used for detecting the remaining erroneous cells after the matrix. Using this code as the final detection stage guarantees a post-decoding undetected block error probability $B_E < 2^{-32} \approx 2 \times 10^{-10}$, regardless of the error before packet decoding.

Next, we turn our attention to the traffic of the network. Fig. 6 investigates the relation between the total traffic intensity ρ and throughput efficiency η. The curves in this figure are produced for two different channels ($p = 10^{-9}$ and $p = 10^{-6}$) and two values of the buffer capacity $K = 16$ and 32. Also shown on the same figure the corresponding intrinsic traffic intensity ρ_0.

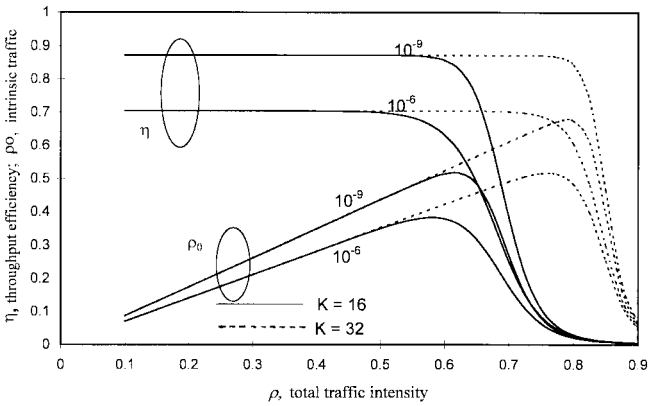

Fig. 6. The effect of total traffic intensity on throughput efficiency and intrinsic traffic.

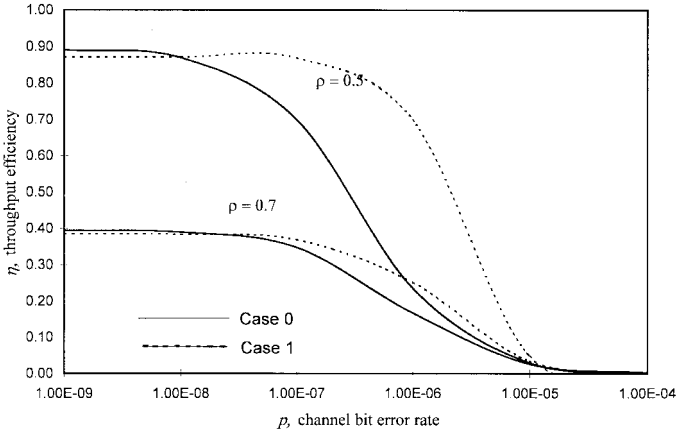

Fig. 7. The effect of checking the payload on the throughput for two values of total traffic intensity.

The linear monotonically increasing part of the ρ_0 - *vs* - ρ curve in Fig. 6 represents the situation where most cells circulating in the network are original cells. That is, the cell-loss probability is very low, and there is hardly any need for retransmission. Over this range, ρ does not affect the efficiency of the system (note the flat part of the efficiency curves). However, attempting to inject more intrinsic traffic to the network, the probability of buffer overflow, and thus the probability of lost cells, increases resulting in a drastic drop of throughput efficiency. The drop in η is directly reflected on ρ_0 which, after reaching a maximum value of $\rho_{0,\max}$, starts to decrease. The value of ρ at which the ρ_0 - *versus* - ρ curve assumes its maximum, call it ρ^*, is the breakpoint between a light network (to the left of ρ^*) and a congested network (to the right of ρ^*). In the figure, $\rho^* = 0.6$ at 10^{-6} and 0.62 at 10^{-9}. The value of $\rho_{0,\max}$ represents the maximum intrinsic traffic that the network can handle. It can be seen that the better channel can withstand a higher $\rho_{0,\max}$ ($\rho_{0,\max} = 0.5$ and 0.35 at 10^{-9} and 10^{-6}, respectively). However, both values are significantly increased to 0.7 and 0.5 by doubling the buffer size to 32. In fact, it was found that increasing the buffer size further to 64 cells phases out any influence of ρ on η.

For the remainder of the paper, the total traffic ρ is kept constant. Consequently, the throughput efficiency η and the carried intrinsic load ρ_0 will be linearly related [see (17)]. Therefore, presenting the results using either terms is equivalent. The rest of the figures are obtained for the throughput efficiency η.

D. Protected Payload versus Unprotected Payload

We next examine the pros and cons of checking the payload. Fig. 7 shows throughput efficiency versus the channel BER when the payload and header are checked (Case 1) and when only the header is checked (Case 0). The efficiency for each case is examined at two values of ρ, namely 0.5 (light network) and 0.7 (congested network). Due to the increased redundancy of Case 1, throughput efficiency is slightly lower than that of Case 0 for very good channels ($p < 10^{-8}$). On the other hand, the effect of redundancy is more than compensated for at higher BER's. This can be explained by recalling that the system in Case 1 yields lower values of $P_E + P_L$ than those in Case 0, or, in other words, higher values of P_C; consequently less retransmissions are requested. The figure shows that the merit of Case 1 over Case 0 diminishes for congested networks ($\rho > \rho^*$).

E. Size of FEC Coding Matrix

The size of the cell-recovery matrix $(M \times N)$ has to be designed to yield the maximum throughput efficiency for a given network.

Let us consider the row size N first. The CLD cell is formatted to handle a maximum value of 16 data cells (i.e. $N = 17$). The CLD cell has the capability of detecting a lost cell independent of the status of the other cells in the row. Therefore B_R is not sensitive to N. It was found that the effect of smaller N on decreasing η (through decreasing α) equals, and in many situations overcomes, its effect on increasing η (through decreasing a). Even when it is advantageous to use a small N to enhance η, the same amount of improvement in η can be obtained by varying M. For these reasons N was set to 17, and the design of the matrix reduces to finding the optimum M. The effect of the network parameters on M are discussed in the following subsections.

F. Channel Quality

To see the effect of p on M, Fig. 8 depicts throughput efficiency versus M for different channels. For good channels ($p < 10^{-7}$), M should be selected to be sufficiently large (>40) to justify the amount of redundancy added by adding one data parity cell per column. However, since the cell-loss probability over such good channels is very low, and hence the retransmissions are very infrequent, the throughput efficiency is not sensitive (flat) for larger values of M.

For poorer channels (for example $p = 10^{-6}$), where the cell-loss probability increases and retransmissions are more frequent, large values of M affect throughput efficiency badly. For the network considered, the value of M that achieves the highest efficiency is around 16. The sensitivity of throughput efficiency to M increases with increasing p.

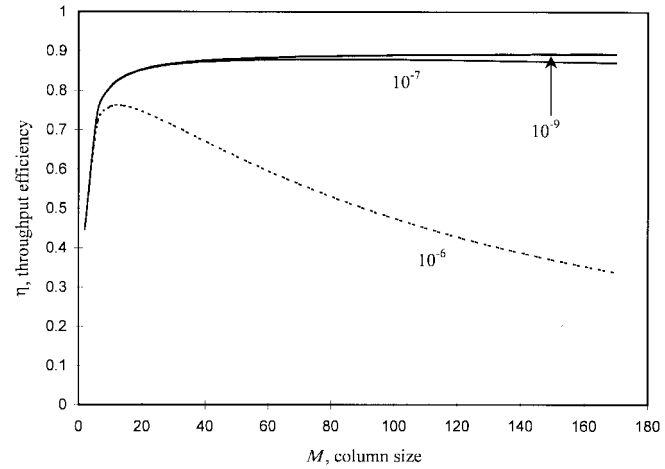

Fig. 8. Studying the effect of the channel BER on the design of M.

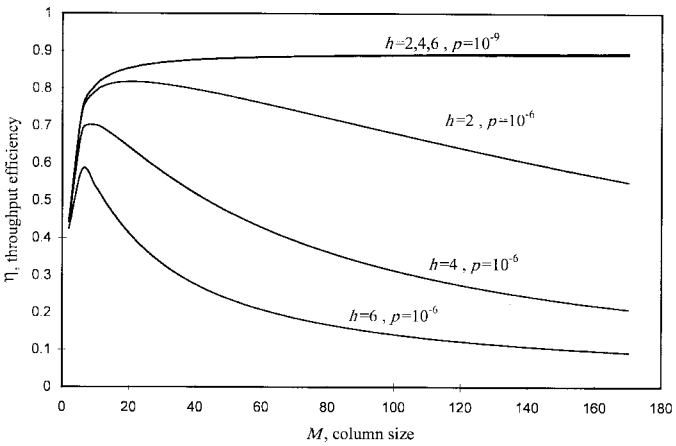

Fig. 9. Studying the effect of the number of hops on the design of M.

G. Number of Hops

The number of hops h affects throughput efficiency through the probability B_R, (as well as the delay a, but to a much lesser degree) and therefore influences the design of M. But, again, for good channels this effect is negligible and the throughput efficiency curves are flat over the range of large M. The throughput starts to become sensitive to an increase in h for poorer channels ($p = 10^{-6}$). Again, the sensitivity of throughput efficiency to M increases with increasing h, as seen in Fig. 9.

H. ARQ Packet Size

The effect of r on the design of M is illustrated in Fig. 10. Two networks with the same parameters except for r have the same post-decoding probabilities. However, the system with longer packets is subject to more transmission errors, and consequently more retransmissions. Therefore increasing r results in decreasing η. (It should be noted that this is valid in our case because the amount of redundancy we are adding for ARQ (32 bits/packet) is negligible. If more overhead is considered, then there will be an optimum value of r). Since increasing M increases the post-decoding cell-loss probability,

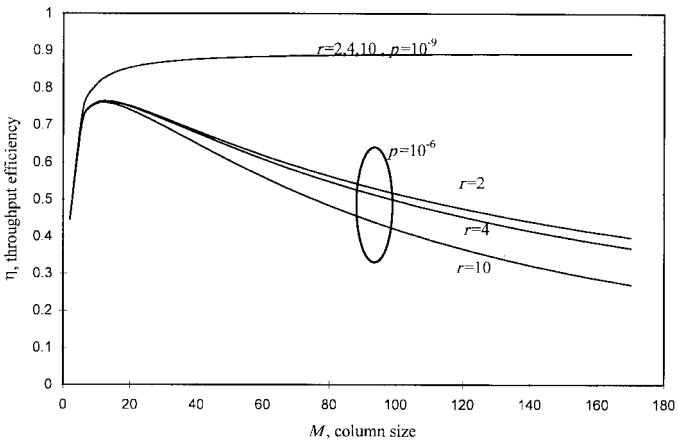

Fig. 10. Studying the effect of the number of cells per packet on the design of M.

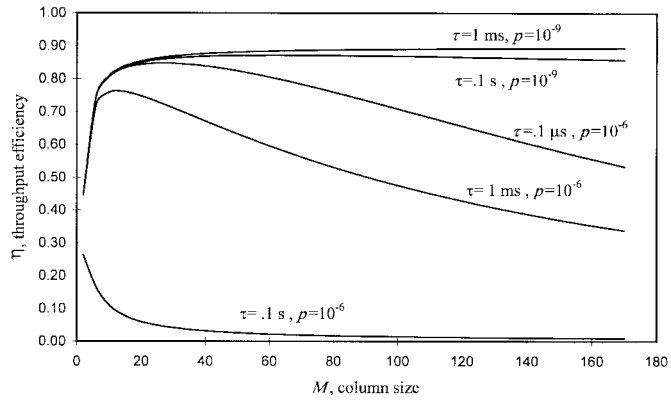

Fig. 11. Studying the effect of the propagation delay on the design of M.

the throughput efficiency is more sensitive to increasing M at large values of r. However, it is interesting to note that the curves for different values of r but the same value of p are identical before reaching the peak. This is so because at such small values of M the probability of having more than one lost cell in a column is very small. As a result, the cell-recovery matrix performs equally well. Consequently, the value of M which achieves the highest throughput efficiency, call it M^*, is not sensitive to r, and all curves reach their peaks at $M^* = 14$.

I. Link Delay

Fig. 11 shows throughput efficiency versus M for three values of τ, namely 10^{-5}, 10^{-3}, and 10^{-1} seconds. The figure helps in finding the optimum of M that maximizes the throughput efficiency for a given delay.

J. Protection of Payload

Figs. 6–11 are obtained for Case 1 (i.e., both data and header are protected). Similar plots were obtained for Case 0. It was found that the dependency of throughput efficiency on M for different p, r or h is less sensitive for Case 0 (e.g., see Fig. 12). However, the sensitivity to M at different delays is the same, as depicted in Fig. 13.

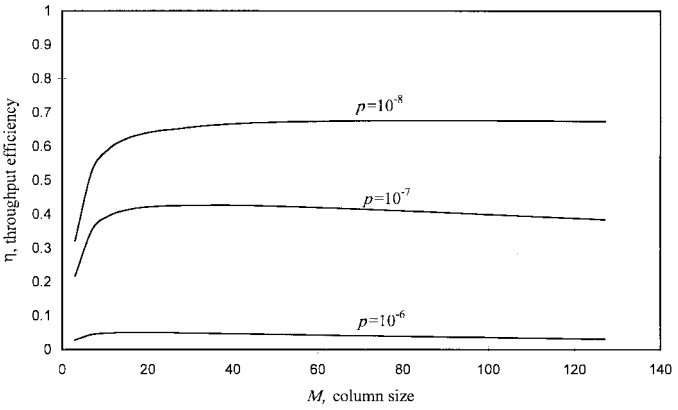

Fig. 12. Studying the sensitivity of the throughput to M when the payload is not checked, for different channels BER's.

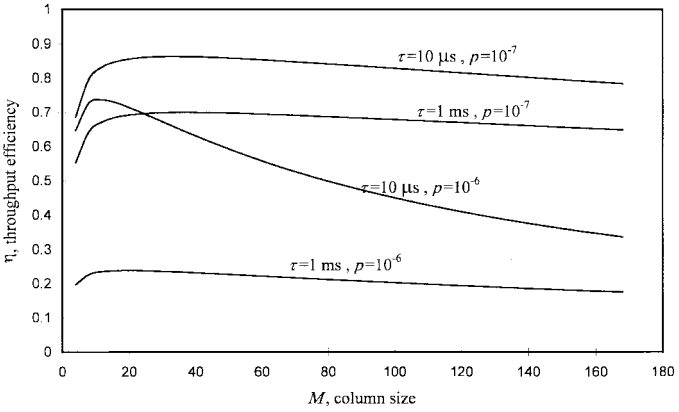

Fig. 13. Studying the sensitivity of the throughput to M when the payload is not checked, for different propagation delays.

V. Case Studies

Let's illustrate how the cell-recovery matrix should be designed taking all network parameters into account. The design will be based on worst-case assumptions, in particular: the worst link BER $(p_{\max})$, the maximum number of hops between any two communicating parties $(h_{\max})$, and the longest propagation delay per link $(\tau_{\max})$. The other parameters are assumed identical. The following networks are considered:

Network 1: $p_{\max} = 10^{-7}$, $h_{\max} = 6$, $\tau_{\max} = 1$;
Network 2: $p_{\max} = 10^{-6}$, $h_{\max} = 2$, $\tau_{\max} = 1$;
Network 3: $p_{\max} = 10^{-6}$, $h_{\max} = 6$, $\tau_{\max} = 0.1$ μ;
Network 4: $p_{\max} = 10^{-6}$, $h_{\max} = 6$, $\tau_{\max} = 1$.

Fig. 14 shows the throughput efficiency for these selected networks. The optimum values of M are 35, 22, 18 and 7, and the maximum efficiency achieved is: 0.85, 0.82, 0.81 and 0.58, respectively.

VI. Conclusion

In this paper, we presented a complete analysis of the error performance of a hybrid ARQ/FEC coding scheme applied to VC of a multihop ATM network. Error detection is performed after each hop, while cell-recovery and request for retransmission are performed at the terminating node. Both options of checking the cell header and the payload

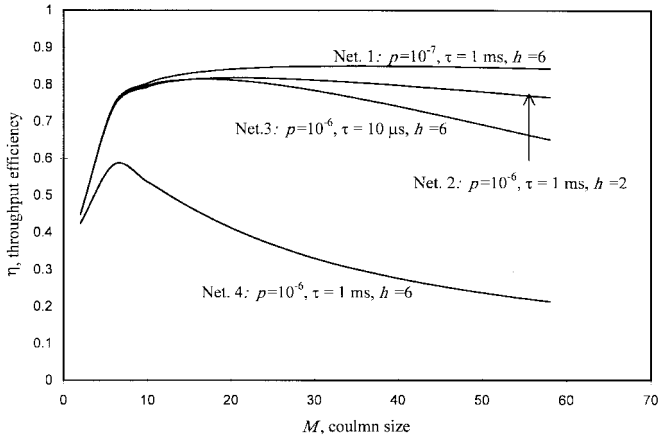

Fig. 14. Study cases.

and checking the cell header only were considered. It was seen that the cell-recovery matrix, although very simple, is very efficient in recovering lost cells. For good channels $(p < 10^{-7})$, and when an ARQ scheme is invoked, it was found that checking the payload is not advantageous. However checking the payload pays off the cost of redundancy very effectively at higher BER. On the other hand, for delay sensitive traffic where retransmissions are not allowed, it is always recommended to check the payload.

In light-traffic networks, most data cells go through the first time they are transmitted, making the probability of retransmission very small. Consequently, the throughput efficiency is very high. As we attempt to increase the carried load beyond a certain amount, the probability of buffer overflow increases and consequently more retransmissions are requested. As a result, the throughput efficiency drops. This sets an upper limit on the maximum intrinsic traffic that can be served. Increasing the queue buffer size helps withstanding higher intrinsic traffic at the cost of increased queueing delay.

Our main emphasis was on designing the dimensions N and M of the cell-recovery matrix. The size of the matrix affects the throughput efficiency in contrary aspects. For example, when the size of the matrix is increased:

1) the efficiency of the FEC matrix increases (hence improving throughput efficiency);
2) the retransmission probability increases (hence deteriorating throughput efficiency);
3) the overall delay increases (hence deteriorating throughput efficiency).

The design is aimed toward finding the optimum size for a given network. As for N (the number of columns), the value $N = 17$ was found to be the most appropriate one to use. The optimum value of M depends on the channel BER, the number of hops, the delay per hop, and the ARQ packet size with different degrees, and therefore has to be designed carefully for a given network parameters. For the case when the header and payload are protected, it was found that the cell-loss probability is increased at a faster rate with increasing M compared to the case when only the header is protected. Therefore, the dependency of throughput efficiency on M for different network parameters is less sensitive for the

latter case. Design curves and study cases were demonstrated for different networks.

ACKNOWLEDGMENT

The authors are very grateful to the editor and reviewers for their useful comments, which improved the presentation considerably. The first author acknowledges King Fahd University of Petroleum and Minerals for supporting this research.

REFERENCES

[1] M. Gerla, T. Y. C. Tai, and G. Gallasi, "Internetting LAN's and MAN's to B-ISDN's for connectionless traffic support," *IEEE J. Select. Areas Commun.*, vol. 11, pp. 1145–1159, Oct. 1993.
[2] I. S. Veniers, J. D. Angelepoules, and G. I. Stassinapoules, "Efficient use of protocol stacks for LAN/MAN-ATM internetworking," *IEEE J. Select. Areas Commun.*, vol. 11, pp. 1160–1171, Oct. 1993.
[3] H. Ohta and T. Kitemi, "A cell loss recovery method using FEC in ATM networks," *IEEE J. Select. Areas Commun.*, vol. 9, pp. 1471–1483, Dec. 1991.
[4] H. T. Lim and J. S. Song, "Cell loss recovery method in B-ISDN/ATM networks," *Electron. Lett.*, vol. 31, no. 11, pp. 848–851, May 1995.
[5] N. Shacham, "Packet recovery in high speed networks using coding and buffer management," in *Proc. IEEE INFOCOM'90 Conf.*, pp. 124–131.
[6] A. R. Kaye, K. Anand, T. Gulliver, and S. Mahmoud, "FEC and priority for VBR video distribution over ATM," *Can. J. Electr. Comput. Eng.*, vol. 19, no. 3, pp. 123–130, July 1994.
[7] J. Simmons and R. Gallager, "Design of error detection scheme for Class C service in ATM," *IEEE/ACM Trans. Networking*, vol. 2, pp. 80–88, Feb. 1994.
[8] S. Lin, D. J. Costello, Jr., and M. J. Miller, "Automatic repeat request error control schemes," *IEEE Trans. Commun.*, vol. 22, pp. 5–17, Dec. 1984.
[9] T. Saadawi, M. A. Ammar, and A. K. Elhakeem, *Fundamentals of Telecommunication Networks*. New York: Wiley, Sept. 1994.

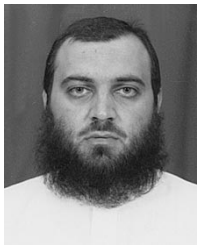

Maan A. Kousa (M'94) received the B.Sc. degree in physics, the B.Sc. and M.Sc. degrees in electrical engineering from King Fahd University of Petroleum and Minerals (KFUPM), Saudi Arabia, in 1985, 1986, and 1988, respectively, and the Ph.D. degree in electrical engineering from Imperial College, London, U.K., in 1994.

He is currently an Assistant Professor with the Department of Electrical Engineering, KFUPM. His research interests are wireless communication, error-control coding, and ATM networks.

Ahmed K. Elhakeem (S'75–M'79–SM'86) received the Ph.D. degree from the Southern Methodist University, Dallas, TX, in 1979.

From 1979–1981, he was a Visiting Professor in Egypt before moving to Ottawa, Canada, in 1982. He assumed research and teaching positions with Carleton and Manitoba Universities and later moved to Concordia University, Montreal, Canada, in 1983, where he is currently a Professor in the Electrical and Computer Engineering Department. He has published numerous papers in IEEE and international journals in the areas of spread spectrum and networking. He is a well-known expert in these areas and serves as a consultant to various companies. His current research interests include wideband networks, switching architectures, CDMA networks, congestion control for ATM-based networks, and ARQ techniques. He is a co-author of the book, *Fundamentals of Telecommunications Networks* (New York: Wiley, 1994).

Dr. Elhakeem has chaired numerous technical sessions for IEEE Conferences and was the Technical Program Chairman for IEEE Montech'86 in Montreal, Canada. More recently, he was the Key Guest Editor for four issues of the IEEE JOURNAL ON SELECTED AREAS IN COMMUNICATIONS on Code Division Multiple Access (CDMA I–IV), appearing in May 1994 and October and December 1996. He is the Communications Chair of IEEE Montreal and TCCC Representative to ICC'99. He currently serves as Associate Editor of the IEEE COMMUNICATIONS LETTERS and is a Professional Engineer of Ontario.

Hui Yang received the Bachelor's degree in major inoptical instrumentation from Beijing Polytechnic University, Beijing, China, in 1988. She is currently pursuing the Master's degree in the Electrical and Computer Engineering Department, Concordia University, Montreal, Canada, while also researching ATM broadband telecommunication.

She was an Assistant Engineer at the Physics Institute, Chinese Science Academy, from 1988 to 1990. Since 1997, she has been a Microwave System Engineer with Nortel Networks, Montreal, Canada.